

1 **Influence of type-I fimbriae and fluid shear stress on bacterial behavior and multicellular**
2 **architecture of early *Escherichia coli* biofilms at single-cell resolution**

3
4 Liyun Wang^{1,3}, Robert Keatch¹, Qi Zhao^{1,#}, John A. Wright², Clare E. Bryant², Anna L. Redmann³,
5 Eugene M. Terentjev^{3,#}
6

7 1: School of Science and Engineering, University of Dundee, Dundee DD1 4HN, UK

8 2: Department of Veterinary Medicine, University of Cambridge, Madingley Road, Cambridge CB3 0ES, UK

9 3: Cavendish Laboratory, University of Cambridge, J. J. Thomson Avenue, Cambridge CB3 0HE, UK
10

11 **Abstract**

12 Biofilm formation on abiotic surfaces in food and medical industry can cause severe contamination and
13 infection, yet how biological and physical factors determine cellular architecture of early biofilms and
14 bacterial behavior of the constituent cells remains largely unknown. In this study we examine the
15 specific role of type-I fimbriae in nascent stages of biofilm formation and the response of micro-colonies
16 to environmental flow shear at single-cell resolution. The results show that type-I fimbriae are not
17 required for reversible adhesion from plankton, but critical for irreversible adhesion of *Escherichia coli*
18 (*E.coli*) MG1655 forming biofilms on polyethylene terephthalate (PET) surfaces. Besides establishing a
19 firm cell-surface contact, the irreversible adhesion seems necessary to initiate the proliferation of *E.coli*
20 on the surface. After application of shear stress, bacterial retention is dominated by the 3D architecture
21 of colonies independent of the population and the multi-layered structure could protect the embedded
22 cells from being insulted by fluid shear, while cell membrane permeability mainly depends on the
23 biofilm population and the duration time of the shear stress.

24 **Keywords:** early biofilms; type-I fimbriae; irreversible adhesion; fluid shear stress.

25 **Introduction**

26 Biofilms are sessile communities of bacteria that grow on solid surfaces, embedded in an extracellular
27 polymeric substance (EPS) matrix (1-3). The biofilm formation generally proceeds via the following
28 steps (1, 4, 5): (i) Planktonic microbial cells approach and then reach the solid surface by Brownian
29 motion, hydrodynamic flow, and active swimming motion. (ii) Once reached, bacteria begin adhering to
30 surfaces. Initially, adherent bacterial cells are attached on the surface reversibly, and many detach to
31 resume the planktonic lifestyle due to the low activation energy for desorption. A fraction of these cells
32 then become irreversibly attached, which might be because bacterial appendages (flagella, fimbriae etc.)
33 overcome the physical repulsive forces of the electrical double layer (6). (iii) The adherent bacteria
34 divide and grow to form micro-colonies on the surface. (iv) Bacteria synthesize a matrix of extracellular
35 polymeric substances, allowing micro-colonies to further develop into mature biofilms, followed by (v)
36 the shed of part of the biofilm to release planktonic bacteria into the surrounding environment.

37 Biofilm formation is a key issue in food industry and in clinical setting. Surfaces infected by biofilms
38 in food-industrial equipment, medical devices and implants could commonly cause illnesses, lethal
39 infections and heavy costs in maintenance (7, 8). Furthermore, when organized into biofilms after
40 maturation, bacteria are resistant to many forms of stress, because EPS is designed to protect embedded
41 bacteria from antibiotics, disinfectants and environmental insults (9). The formation of biofilms
42 therefore has been intensively studied, especially in terms of dynamics of adhesion process and genes
43 involved in EPS production, as well as regulatory mechanisms and overall morphology of mature
44 biofilms (9, 10). Nevertheless, in order to provide a better insight into mechanisms underlying biofilm
45 formation, the nascent stages of biofilm development (i.e., adhesion and proliferation) need to be further
46 elaborated at single-cell resolution.

47 Macroscopic biofilm formation is dramatically affected by bacterial properties (e.g. cell appendages)
48 and environmental factors (e.g. fluid shear). For instance, deficient fimbriae would alter the morphology

49 of biofilms (11) or lead to a defective biofilm formation (12); fluid shear could cause biofilm breakage
50 (13) and deformation (14). However, at single-cell resolution, although the critical role of fimbriae/pili
51 in bacterial adherence to abiotic surfaces has been extensively studied over the past two decades, little is
52 understood about their effect on the proliferation stage of biofilm formation (step (iii)), and few studies
53 focus on the responses of early biofilms to fluid shear stress including cell membrane permeability and
54 multicellular architecture. Usually, the effect of shear stress on bacterial adhesion and macroscopic
55 biofilm morphology on abiotic substrates is investigated using bacteria suspended in the fluid, which
56 could reveal how the flow affects biofilm formation when surfaces are exposed to bacteria-existed
57 environment, e.g. ships in the sea and catheters in contaminated urine. These cells are allowed to attach
58 or grow on the immersed surface under different flow regimes, in which shear stress might: increase
59 bacterial adhesion due to mass transport, prevent bacterial attachment and remove bacteria that are
60 already bound (15-18). In contrast to our study, early biofilms grown on PET substrates were statically
61 incubated before the application of shear stress, thus rendering it possible to just focus on how fluid
62 shear influences bacterial behavior during the nascent stages of biofilm formation, which could mimic
63 cleaning in place (CIP) procedures for food processing equipment (19) and uncover how contaminated
64 surfaces of medical devices and implants are affected by flow fluids.

65 Previously we presented architectural transitions in *E.coli* MG1655 biofilms on PET surfaces over the
66 early stages of formation (steps (i) - (iii) on the list above) at single-cell resolution (20). These changes
67 revealed the dynamics, and the structural principle by which individual cells developed into micro-
68 colonies. We obtained the 'growth curve' of adhering cells, which exhibited distinct lag and log phases.
69 It is worth noting that the generation time in the log phase (step (iii)) was more than twice as long as that
70 of planktonic counterparts under the same incubation conditions, which was not due to the detachment
71 of the daughter cells back into the bulk medium - but purely due to extra expenditure for cells to remain
72 adhered on the surface. We found that the 3D cellular architecture of early biofilms could influence

73 biological processes (e.g. quorum sensing) and physical properties (e.g. interactions between cells and
74 cells/substrates) of the constituent bacteria. PET is the substrate of choice since it is ubiquitous in food
75 packaging and widely used in cardiovascular implants (e.g. vascular grafts) due to its excellent
76 physicochemical properties: good mechanical strength, stability in the presence of body fluids, and
77 relatively high biocompatibility (21, 22).

78 Here, we examine the influence of type-I fimbriae by comparing the growth of adherent *E.coli*
79 MG1655 mutants that lack type-I fimbriae - *E.coli* appendages facilitating the attachment, and the effect
80 of fluid shear stress on bacterial behavior and cellular architecture of *E.coli* micro-colonies. We will
81 clarify the specific role of type-I fimbriae in the initial adhesion of *E.coli* and in the subsequent growth
82 into colonies on surfaces, and find how cell behavior is affected when the collective architecture of
83 micro-colonies is challenged by fluid shear.

84 **Materials and Methods**

85 **Substrate.** PET plates with a thickness of 0.35 mm and low roughness ($R_a = 5 \pm 0.2$ nm) were
86 purchased from Goodfellow Cambridge Ltd. (Huntingdon, UK). The plates were cut into small pieces
87 (21.5 mm \times 8 mm) and cleaned ultrasonically in absolute ethanol for 15 min and then in deionized
88 purified water for 15 min. They were then dried with nitrogen.

89 **Bacterial strains, media, culture and mutant strain construction.** The wild-type *E.coli* MG1655
90 was cultured in Luria broth (LB) medium, and its mutants that lack the major subunits of type-I fimbriae
91 applied in this study to assess the biofilm behavior of cells with defective fimbriae was incubated in LB
92 medium with 100 μ g/mL kanamycin.

93 A single colony of a strain was inoculated into a test tube containing 5 mL of culture medium and
94 grown overnight at 37 °C, with agitation at 200 rpm. A 100 μ L of this culture was transferred into a fresh
95 tube of 5 mL medium and incubated with shaking until the stationary phase was reached (12 to 14 h) to
96 obtain the eventual microbial suspension, which contained $\sim 10^9$ colony-forming units per mL

97 (CFU/mL).

98 *E. coli* MG1655 $\Delta fimA::kan$ mutant strain (abbreviated as $\Delta fimA$ mutants in the text) was constructed
99 by oligo-directed mutagenesis (ODM) as described previously (23). Briefly, PCR was used to amplify a
100 kanamycin resistance cassette from the plasmid pBADkanFRT using oligonucleotides specific to the
101 cassette, which have 5' 60bp arms homologous to DNA directly flanking the gene of interest, using
102 primers 947 (aaagtgtacagaacgactgccatgtcgatttagaaatagtttttgaaggaaagcagctaggataggcttacctcaagctc)
103 and 948 (atTTTTatcgcaacaagggtgggcatccctgcccgaatgacgtccctgaacctgggtaggatgacgatgacaagctcccccttctg).
104 *E. coli* MG1655 containing the pBAD λ Red plasmid was grown in LB medium containing 100 μ g/mL
105 ampicillin at 37°C, 200rpm to an OD₅₉₅ of 0.25. Expression of the red recombinase genes was induced
106 by the addition of L-arabinose to a final concentration of 0.2% w/v. Cultures were incubated further until
107 an OD₅₉₅ of 0.5 was reached, and electrocompetent cells were prepared. Purified PCR products were
108 used to electroporate the cells, and mutant colonies were selected on LB agar plates containing 50
109 μ g/mL kanamycin. Successful allelic replacement of *fimA* was confirmed by PCR and sequencing using
110 primers 1065 (ctatgagtcaaaatggcccca) and 1066 (agagcctgaataaagccgttt). The pBAD λ Red plasmid was
111 cured by serial passage in the absence of antibiotic selection. Given that *fimA* is found within an
112 operon of 9 genes involved in the biogenesis of type-I fimbriae, any polar effects of the *fimA* deletion
113 would only influence other type-I fimbrial genes. Thus, we are confident that the observed phenotype is
114 due to the loss of type-I fimbriae.

115 **Bacterial adhesion and growth on PET surfaces.** The samples were prepared by following the
116 procedures reported previously (20), with slight modifications. Briefly, sterilized PET surfaces were
117 rinsed thrice with sterile water and then with LB medium. Each substrate was then placed vertically into
118 a test tube (diameter, 22 mm) containing stationary-phase *E. coli* MG1655 or $\Delta fimA$ mutant cells
119 suspended in LB culture at 37 °C for 1 h, to carry out the initial adhesion. Three of the samples were
120 subsequently taken out for Confocal Laser Scanning Microscopy (CLSM; LEICA TCS SP5) imaging

121 and another nine (three replicates for each fluid shear stress) were taken for fluid shear experiments. The
122 other 'seeded' PET plates with wild-type or mutant cells were subjected to the following incubation
123 process with refreshed LB medium.

124 The incubation process: The remaining 'seeded' PET plates were gently rinsed twice with 10 mL pre-
125 warmed fresh LB medium, before being individually immersed into a new tube containing 5 mL pre-
126 warmed fresh LB medium at 37 °C for 1 h. After each consecutive hour of incubation, three of the
127 samples were taken out for the CLSM imaging and another nine (three replicates for each fluid shear
128 stress) were taken for fluid shear experiments, but all other remaining plates were subjected to the
129 incubation process again.

130 In order to investigate the effect of quorum sensing and multiple-layer architecture on the response of
131 constituent bacteria in micro-colonies to the fluid shear stress, nine of the samples with 'seeded' *E.coli*
132 MG1655 on substrates were incubated with hourly-refreshed LB medium containing 1.56 mg/L (Z-)-4-
133 Bromo-5-(bromomethylene)-2(5H)-furanone (FC 30, Sigma-Aldrich, UK) for 8 h. FC 30 is a quorum
134 sensing inhibitor (signal antagonist), and it can compete with the quorum sensing signal molecules for a
135 common binding site on LuxR-type transcriptional activators, which are responsible to regulate
136 expression of target genes for the subsequent quorum sensing (24, 25). In our previous research (20), we
137 found at this concentration of FC 30, bacterial quorum sensing was inhibited but the growth rate was not
138 affected. These nine treated samples (three replicates for each fluid shear stress) were then challenged by
139 fluid shear.

140 **CLSM imaging.** In a comparison with the adhesion and growth of *E.coli* MG1655 on PET surfaces,
141 which have been previously elaborated (20), surface samples with mutant cells were gently washed with
142 tris-buffered solution (TBS) thrice, stained with the BacLight Live/Dead viability kit (Invitrogen, kit no.
143 L7007) for 15 min in the dark and then visualized using Confocal Laser Scanning Microscopy (LEICA
144 TCS SP5) with an oil-immersion objective lens at 40 × magnification, zoom 1:2.60 or 1:1.00. In CLSM

145 images, green and red stained cells could indicate membrane permeability status: green cells have intact
146 membranes, and red cells are membrane compromised (i.e. membranes are permeable or damaged).

147 **Fluid shear experiments.** A special vibration device was built to detach bacteria by a shear force
148 produced in oscillatory flow. This differs from other techniques (e.g. with rotating disk (26)) where the
149 shear force is consistent in one direction, enabling cells to adapt and develop resistance. In our case,
150 oscillations at high frequency create an essentially random force on ‘unprepared’ cells, and probe the
151 strength of their natural attachment. In order to expose bacteria to this shear force, samples were glued
152 onto a holder, which was vibrated horizontally in a dish filled with phosphate-buffered solution (PBS).
153 The dish was kept at 37 °C to produce optimal conditions for bacteria. The vibrational movement was
154 produced by a mechanical setup, which moves two magnets underneath the dish by a mechanism
155 converting rotational movement into a horizontal linear motion. The frequency of this motion can be
156 adjusted to different values between 5Hz and 25Hz. The moving magnets were locked to two reciprocal
157 magnets embedded in the sample holder, thus allowing the movement of the sample holder in the dish
158 without any leakage of liquid. The holder vibrated along one axis in the plane of the dish, because its
159 movement was constrained by a track-like excavation in the dish. The shear stress acting on the bacteria
160 on the surface, moving with respect to a stationary fluid above, is a function of vibration frequency. An
161 expression for this stress can be analytically calculated by considering the hydrodynamics around an
162 oscillatory plate in liquid, producing $f_{max} = -r\omega^{3/2}\sqrt{\rho\eta} \cdot A$, where f_{max} is the maximal force acting
163 on the cells during vibration, r is the amplitude of vibration, ω is the angular frequency of vibration
164 [rad/s], ρ and η are the density [kg/m³] and viscosity [Pa.s]. Finally, $A \approx 0.5 \mu\text{m} \times 3 \mu\text{m}$ is the average
165 surface area of the *E.coli* cell. In our experiments, we worked with the shear stress values of 0.58 Pa,
166 1.45 Pa and 3.30 Pa (referred to for convenience as low, medium and high stress in the following text),
167 which translate to the maximum force amplitude of 0.87 pN, 2.18 pN and 4.95 pN, respectively. These
168 shear stresses are comparable to the wall shear stress (WSS) in medical devices e.g. hemodialysis

169 vascular access (WSS applied mainly ranges from 0.1 to 3 Pa) (27) and central venous catheters (WSS
170 applied mainly ranges from 0 to 1.8 Pa) (28), and those generally used in CIP procedures for food
171 processing equipment (WSS applied in pipes mainly ranges from 0 to 3 Pa) (19).

172 The surface samples with ‘seeded’ *E.coli* MG1655 or $\Delta fimA$ mutant cells and those with bacterial cells
173 statically incubated after each consecutive hour were treated by fluid shear stresses, and then stained and
174 visualized by CLSM.

175 **Image processing.** Images were processed using ImageJ software (NIH, Bethesda, Maryland,
176 <http://rsbweb.nih.gov/ij/>) to quantitatively determine the number of wild-type/mutant cells on surfaces
177 (i.e. cell density, cells/mm²) and the cell size (i.e. area of the individual cell μm^2). For each sample, 20
178 fields of view were randomly chosen, and the whole measurement process was repeated three times
179 independently, i.e. a total of 60 values for each cell density. The fraction of cells remaining on substrates
180 is the ratio of cell density after shear stress was applied and the density in the control sample without
181 shear treatment. The fraction of cells with intact membranes is the ratio of the cell density of green cells
182 and that of total cells remaining on surfaces.

183 The above experiment process was repeated three times independently. All statistical analysis was
184 performed using ANOVA testing within Microsoft Excel (Microsoft Corp., Redmond, WA). Values were
185 reported in the text as mean value \pm standard deviation.

186 **Results**

187 **The adhesion and growth of $\Delta fimA$ mutants on surfaces.** After 1 h incubation of PET substrates with
188 $\Delta fimA$ mutant suspension (i.e. the start point of incubating surface samples with fresh LB medium,
189 labelled as 0 h), the CLSM images (Fig. 1) reveal that the densities of ‘seeded’ mutant cells and ‘seeded’
190 *E.coli* MG1655 cells are $(6.4 \pm 0.7) \times 10^2$ cells/mm² and $(6.1 \pm 0.9) \times 10^2$ cells/mm², respectively. It could
191 be seen that there is no significant difference observed in this initial adhesion between non-fimbriated
192 cells and wild-type cells. Following the first 2 h incubation of ‘seeded’ cells on substrates with sterile LB

193 medium, Fig. 2 illustrates that the numbers of *ΔfimA* mutants and of *E.coli* MG1655 cells on the surface
194 both decreased with incubation time. Meanwhile, over this 2 h incubation, the cell size of individual
195 adherent *ΔfimA* mutants increased from $2.1 \pm 0.3 \mu\text{m}^2$ to $5.6 \pm 0.4 \mu\text{m}^2$ ($P < 0.005$), as the wild-type cells
196 did from $2.3 \pm 0.4 \mu\text{m}^2$ to $5.7 \pm 0.5 \mu\text{m}^2$ ($P < 0.005$).

197 However, the behavior of adherent non-fimbriated *E.coli* was totally different from that of wild-type
198 cells hereafter: after 2 h, the apparent number of surface-bound wild-type cells stopped decreasing and
199 then began to exponentially grow on the surface, while the attached mutants continued detaching from
200 the surface with incubation time until adherent fimbriae mutants could hardly be seen in any field of
201 view at 6 h (Fig. 1), suggesting that non-fimbriated cells remained reversibly attached on the substrate
202 by purely physical interactions.

203 **The effect of fluid shear stress on micro-colonies.** To elaborate the effect of the shear on the cellular
204 response of early biofilms, the *E.coli* MG1655 growing on PET substrates which exhibits three stages -
205 ‘singles’ (only single cells could be observed in the field of view, i.e., lag phase), ‘single-layer clusters’
206 and ‘multi-layer colonies’, were treated with different fluid shear stresses. Figure 3 shows that apart
207 from the altered architecture resulting from bacterial detachment, the cellular response of constituent
208 bacterial cells in micro-colonies to shear stress should include cell membrane permeability.

209 Figure 4 summarizes bacterial detachment and cell membrane permeability due to the shear stress
210 treatment. It could be seen from Fig. 4a that higher shear stress acting on adhering bacteria led to lower
211 bacterial remaining population at the same incubation time point, which is consistent with previous
212 literature (15), and that the amount of cells remaining on surfaces increased with bacterial progressing
213 colonization. During the first 2 h incubation when the single cells were in the lag phase, all of attached
214 cells could be removed by high shear stress, while the fraction of remaining bacteria gradually rose from
215 $20\% \pm 8\%$ at 0 h to $55\% \pm 8\%$ at 2 h under medium shear stress, implying that reversibly ‘seeded’ wild-
216 type *E.coli* were being irreversibly immobilized on PET surfaces over this period. The ‘seeded’ mutant

217 cells on PET substrates (i.e. samples at 0 h) and the adherent mutants on surfaces after the first 1 h or 2 h
218 incubation, were flushed by fluid at the medium shear stress (1.45 Pa) for only 10 s. Compared with
219 wild-type *E.coli*, all of adherent mutants on each surface sample were removed after fluid shear
220 treatment, confirmed by the CLSM images (data not shown). From 3 to 6 h when adhering wild-type
221 bacteria were exponentially growing into single-layered micro-colonies, the bacteria staying on surfaces
222 after being treated by medium and high shear stresses respectively maintained at the level of
223 approximately 83% and 40%. After 7 h when multiple-layer architecture of colonies emerged, the
224 bacterial retention under medium and high shear sharply increased to above 92% and around 80%,
225 respectively. The effect of fluid shear on the bacterial cell membrane permeability is shown in Fig. 4b.
226 Similar to the detachment, Fig. 4b illustrates that higher shear stress also caused lower fraction of cells
227 with intact membranes at the same incubation time point. However, the cell membrane permeability kept
228 constant until the end of ‘single-layer clusters’ stage (6 h). When clustered bacteria developed into
229 multiple-layer colonies after 7 h, for surfaces exposed to medium and high shear stresses, the fractions
230 of cells with intact membranes on surfaces increased from the level of 45% to above 99% and from the
231 level of 30% to above 80%, respectively.

232 To determine whether the multiple-layer architecture or the larger population results in such increased
233 bacterial retention and cell membrane integrity after 6 h incubation, *E.coli* MG1655 growing on PET
234 substrates were incubated with LB culture medium containing quorum sensing inhibitor (FC 30) at a low
235 concentration for 8 h. Based on our previous study (20), the bacterial growth rate would not be affected
236 in this situation, i.e. the number of cells at each hour interval would be same as counterparts without
237 inhibition of quorum sensing, but the multi-layered structure could not form with suppressed quorum
238 sensing, and colonies were therefore remained as large single-layered clusters after 8 h incubation (Fig.
239 5). Compared with the 8 h-samples without FC 30 treatment, the fractions of quorum sensing-inhibited
240 bacteria remaining on surfaces after application of medium and high shear stress both decreased to their

241 levels at ‘single-layer clusters’ stage (i.e. around 83% and 40%, respectively), and the corresponding
242 fractions of cells with intact membranes respectively declined to $96\% \pm 1\%$ and $58\% \pm 4\%$, which were
243 still significantly higher than their corresponding samples with incubation of less than 6 h (both P values
244 were less than 0.005).

245 To characterize how duration time of shear stress influences bacterial detachment and cell membrane
246 permeability, the original exposure time (120 s) was either shortened to 40 s or extended to 360 s. This
247 effectively tests the total mechanical energy delivered to cells over this time period, as opposed to
248 merely testing the detachment force. The surface samples with *E.coli* MG1655 growing for 5 h and 8 h
249 were chosen for this test. For 5 h-incubation samples, as shown in Fig. 6a, with the increase of duration
250 time, the amount of remaining bacteria slightly declined in the presence of medium fluid shear, while it
251 dramatically fell off from $67\% \pm 5\%$ to $14\% \pm 5\%$ ($P < 0.005$) when high shear stress was applied.
252 Although the longer duration of medium shear stress could hardly stimulate bacterial detachment, it led
253 to a rapidly decrease in the fraction of cells with intact membranes from $65\% \pm 5\%$ to $15\% \pm 3\%$
254 ($P < 0.005$), as the high shear stress did from $44\% \pm 6\%$ to $5\% \pm 2\%$ ($P < 0.005$) (Fig. 6b); For 8 h-
255 incubation samples, Figure 6 shows that the stimulating effect due to the extension of acting time on the
256 detachment and cell membrane permeability is much smaller than that exhibited on the surface with
257 single-layered colonies.

258 Discussion

259 **The role of type-I fimbriae in *E.coli* early biofilm formation.** Type-I fimbriae are generally
260 considered to be necessary for the initial adhesion of *E.coli* on abiotic surfaces, since the fimbrial mutant
261 of *E.coli* was widely reported to be defective in the initial attachment on abiotic surfaces. For instance,
262 Pratt and Kolter incubated polyvinylchloride (PVC) surfaces with diluted bacterial suspension in LB for
263 24 h, and found that type-I fimbrial mutants of *E.coli* were hardly attached (12). Cookson et al.
264 demonstrated that compared with the wild-type *E.coli*, the adherence of type-I fimbrial mutants to

265 surfaces was reduced by 45% after incubation in LB broth for 48 h (29). However, such a long period of
266 culture in the closed system could introduce bacterial detachment from and reattachment back onto the
267 surface, thus rendering it ambiguous whether this change in adhesion is due to the defective adhering
268 ability of mutants or to the detachment after reversible adhesion. In this study, we measured the number
269 of adherent *E. coli* MG1655 $\Delta fimA$ mutant cells on PET surfaces over time and the external medium in
270 which the PET surfaces were incubated was refreshed each hour to maintain a constant culturing
271 environment. Thus, in our case the continuous recruitment of new cells from the incubation medium
272 onto surfaces was deliberately avoided, to allow us finding the specific role of type-I fimbriae in the
273 initial reversible or irreversible adhesion of *E. coli*, and in the subsequent growth on surfaces.

274 The adhesion assays in which PET substrates were incubated with bacterial suspensions indicate that
275 mutant cells, which lack the type-I fimbria structure, could reach a surface equally well, and then
276 normally undergo the initial attachment. That is, type-I fimbriae of *E. coli* appear to be unnecessary for
277 the ‘cell to surface’ phase of step (i) described in the Introduction. Moreover, the detachment over the
278 first 2 h incubation under unstressed condition reveals that the initially ‘seeded’ cells of wild-type and
279 non-fimbriated *E. coli* were both reversibly attached on PET surfaces with a low barrier for desorption.
280 Hence, the similar amounts of initially adherent cells of both strains suggest that type-I fimbriae may be
281 not an essential factor in the reversible adhesion of *E. coli* to surfaces. Instead, the bacterial surface and
282 the flagella may facilitate the reversible cell-surface contact.

283 The wild-type cells stopped detaching from the surface at the end of lag phase (0-2 h), and more than
284 half of cells could remain surface-bound after medium shear stress treatment, suggesting that after the
285 lag phase the adherent wild-type cells completed transition from reversible to irreversible adhesion.
286 However, the further detachment of adherent $\Delta fimA$ mutants with the increase of incubation time under
287 unstressed condition shows that non-fimbriated *E. coli* could not achieve a stable cell-surface attachment
288 (i.e., become irreversibly attached). Thus, we could demonstrate that type-I fimbriae are of importance

289 to the irreversible adhesion of *E.coli* on abiotic surfaces. It also indicates that the defect in the initial
290 attachment of fimbrial mutants described in the previous literature (12, 29) may be due to the
291 detachment after adhesion, not to the deficient ability in the reversible attachment.

292 During the lag phase, the adhered bacteria of both strains did not replicate but dramatically increased
293 in size. This is because the initially attached cells on the surface need to synthesize the enzymes and
294 factors needed for cell division under the new environmental conditions (20, 30). For example, the
295 average intracellular concentration of FtsZ (the major cytoskeletal protein during binary fission) in
296 *E.coli* was found to remain constant over the course of the cell cycle, thus bacteria in the lag phase
297 delayed division until they achieved a size with sufficient levels of FtsZ to replicate on surfaces (31, 32).
298 Compared with wild-type counterparts, surprisingly, reversibly attached non-fimbriated cells could not
299 form any cluster after the lag phase. Therefore, it appears that bacterial transition from reversible to
300 irreversible adhesion is quite vital to the initiation micro-colony formation. One possible explanation is
301 that the irreversible attachment mediated by type-I fimbriae would lead to an alteration in the
302 composition of outer membrane proteins of *E.coli* (33), which might trigger the subsequent growth and
303 colony formation. The *ΔfimA* mutants that lack type-I fimbriae could only maintain reversible
304 attachment, thus these adherent non-fimbriated *E.coli* cannot progress into the next stage to grow on the
305 surface.

306 From the above discussion, it is clear that irreversible adhesion is required to initiate the colonization
307 of adherent bacteria on substrates. The irreversibly adherent parent bacteria would divide by undergoing
308 elongation and subsequent separation during which the parent cell and the new daughter *E.coli* would
309 utilize type-I fimbriae to stay irreversibly bound to the surface. By this means, bacterial irreversible
310 attachment on the substrate could be passed on to the next generation. This may explain why the genes
311 encoding structural components of type-I fimbriae were found up-regulated in the biofilm cells (12, 34).
312 Moreover, this also reminds us of the issue that the doubling time in the log phase of attached *E.coli*

313 (~38 min) was more than twice as long as that of planktonic cells (~16 min) under the same incubating
314 condition, which was found in our previous research (20). Different from the proliferation of freely
315 swimming bacteria in liquid medium, newborn daughter cells of surface-bound bacteria may need some
316 time to complete irreversible attachment, thus this time would prolong the doubling time of sessile cells
317 growing on surfaces, which might be the reason for this issue.

318 **The responses of early biofilms to fluid shear stress.** The fluid flow acting parallel to a substratum
319 surface would generate shear stress. When the shear forces overcome the adhesive forces anchoring cells
320 onto the abiotic substrate, the fluid flow may cause adhering bacteria to slide and roll over the surface,
321 potentially detaching them from substrates (16, 35). It could be clearly seen from the 8 h-samples in Fig.
322 3 that the shear flow led to morphological changes in the cellular architecture of micro-colonies through
323 bacterial migration and detachment. The large compacted multi-layered colonies were migrated into
324 loose smaller groups under medium shear stress, and the constituent cells especially those in the upper
325 layer were detached from surfaces under high shear.

326 The fraction of remaining bacteria, which can quantitatively reveal interaction forces between bacteria
327 and substratum surfaces (5, 36), was strongly dependent on the growing phases of *E.coli* cells before
328 they were challenged by the fluid flow. When cells were in the ‘lag phase’, i.e. ‘singles’ stage, although
329 these adherent cells did not start to divide, their binding forces with surfaces were stronger with the
330 increase of incubation time; After the population entered the log phase, the resulting single-layered
331 colonies showed much higher ability to resist removal by shear than the single cells in the lag phase.
332 During the stage of ‘single-layer clusters’, we found the interaction between colonized bacteria and
333 substrates did not increase with the development of micro-colonies, different from bacteria-host tissue
334 interaction which increased with bacterial population during the initial growing on tissue surfaces (37).
335 Instead, it maintained at the same level under the given shear stress until the occurrence of multi-layered
336 colonies when the interaction significantly increased. Combined with the results regarding 8 h-samples

337 with quorum sensing inhibited (single-layered colonies containing an equal amount of cells with the
338 multi-layered still displayed the fraction of remaining cells shown in the stage of ‘single-layer clusters’),
339 it could be concluded that the attachment strength of early biofilms is concerned with the population but
340 with the 3D architecture of micro-colonies, and the multiple-layer structure of biofilms could protect the
341 embedded cells from being insulted by fluid shear, which might be due to the formation of EPS (3, 9).

342 The effect of duration time of shear stress on bacterial retention was found to rely on the relative level
343 of the given shear force and bacterial adhesive force. If the flow shear force was lower than the adhesive
344 force of most of bacteria in the micro-colonies, few loosely attached bacteria would be immediately
345 detached after application of the flow, but the rest of cells would tend to stay on surfaces independent of
346 the periods loading shear stresses. When the applied shear stress was quite high to remove the adhering
347 cells in the colonies, an increase of duration time of the shear would yield a higher bacterial removal
348 from surfaces.

349 Although bacteria are protected by a rigid cell wall composed of peptidoglycans, the external
350 hydrodynamic stress would result in damage inflicted on bacterial cell surface (38-40), however few
351 studies exist on bacterial membrane damage in biofilms caused by flow shear. In this work, by staining
352 cells with a viability kit, the response of cell membrane permeability in micro-colonies to fluid shear
353 was investigated. The cell membrane permeability after medium shear stress treatment kept constant
354 during 0-2 h, i.e., the permeability was not affected by bacterial transition from reversible to irreversible
355 adhesion, which reveals that this effect was independent of bacterial binding strength with substrates.
356 Different from the results on bacterial retention, the permeability was mainly dependent on the
357 population of colonies: The fraction of cells with intact membranes would be kept constant until the
358 amount of constituent cells in micro-colonies was above some critical level. Then the cell membrane
359 integrity after shear treatment increased with the population, even when the 3D architecture of colonies
360 was inhibited by quorum sensing inhibitor. It appears that the multi-layered architecture was able to

361 protect cell surface from damaging due to high flow shear. Moreover, cell membrane permeability in
362 early biofilms was found to be time-dependent regardless of the magnitude of shear stress in the
363 environment.

364 **Conclusions**

365 In this study, we clarify that the type-I fimbriae could facilitate the irreversible adhering process of
366 daughter cells during the exponential phase of early biofilm formation, and after surface-bound bacteria
367 enter the proliferation phase to form micro-colonies, they would be difficult to detach. When quorum
368 sensing is inhibited, the interaction between bacteria in micro-colonies and substrates and the cell
369 membrane of constituent cells are more vulnerable to high shear stress, which suggests that fluid flow
370 shear could be combined with the application of cell signaling inhibitor to remove bacterial
371 contamination on surfaces.

372

373 **Acknowledgments**

374 Financial support from Engineering and Physical Sciences Research Council (EPSRC, EP/P00301X/1)
375 and Unilever Corporate Research is acknowledged.

376

377 **References**

- 378 1. **Stoodley P, Sauer K, Davies D, Costerton JW.** 2002. Biofilms as complex differentiated
379 communities. *Annu Rev Microbiol* **56**:187-209.
- 380 2. **Flemming H-C, Wingender J.** 2010. The biofilm matrix. *Nat Rev Microbiol* **8**:623-633.
- 381 3. **O'Toole G, Kaplan HB, Kolter R.** 2000. Biofilm formation as microbial development. *Annu*
382 *Rev Microbiol* **54**:49-79.
- 383 4. **Anselme K, Davidson P, Popa A, Giazzon M, Liley M, Ploux L.** 2010. The interaction of cells
384 and bacteria with surfaces structured at the nanometre scale. *Acta Biomater* **6**:3824-3846.

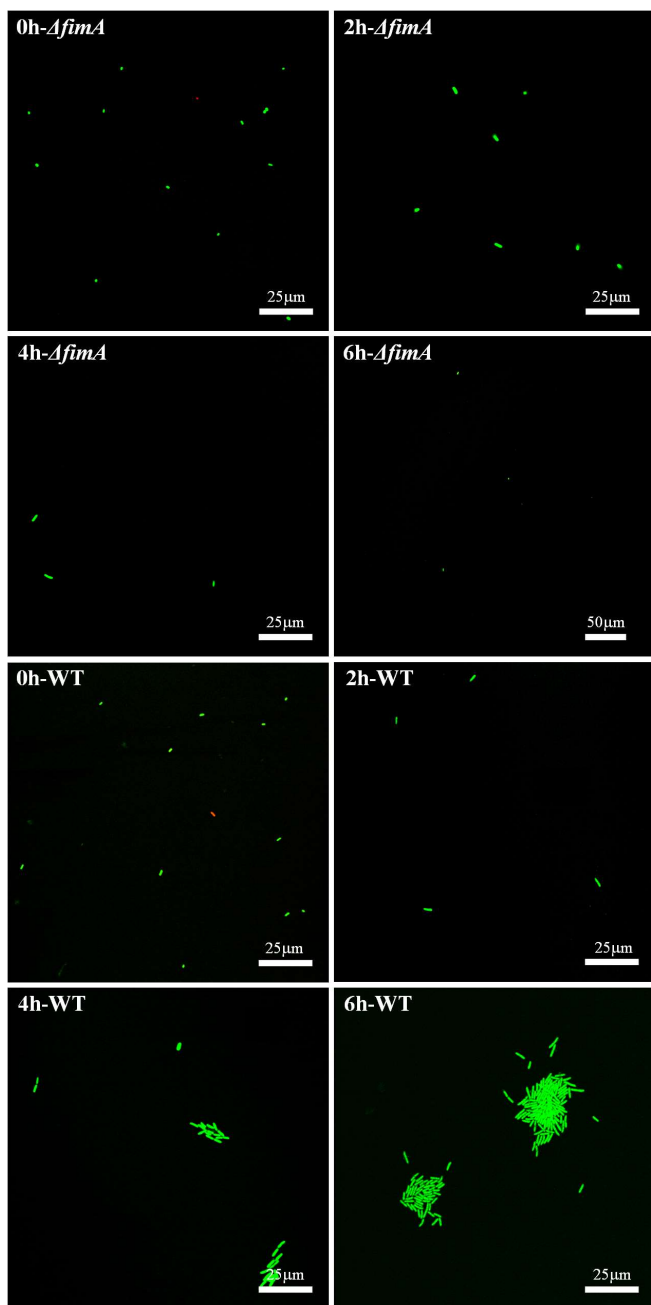
- 385 5. **Katsikogianni M, Missirlis Y.** 2004. Concise review of mechanisms of bacterial adhesion to
386 biomaterials and of techniques used in estimating bacteria-material interactions. *Eur Cell Mater*
387 **8.**
- 388 6. **Garrett TR, Bhakoo M, Zhang Z.** 2008. Bacterial adhesion and biofilms on surfaces. *Prog Nat*
389 *Sci* **18**:1049-1056.
- 390 7. **Costerton J, Montanaro L, Arciola C.** 2005. Biofilm in implant infections: its production and
391 regulation. *Int J Artif Organs* **28**:1062-1068.
- 392 8. **Davey ME, O'toole GA.** 2000. Microbial biofilms: from ecology to molecular genetics.
393 *Microbiol Mol Biol R* **64**:847-867.
- 394 9. **Branda SS, Vik Å, Friedman L, Kolter R.** 2005. Biofilms: the matrix revisited. *Trends*
395 *microbiol* **13**:20-26.
- 396 10. **Drescher K, Dunkel J, Nadell CD, van Teeffelen S, Grnja I, Wingreen NS, Stone HA,**
397 **Bassler BL.** 2016. Architectural transitions in *Vibrio cholerae* biofilms at single-cell resolution.
398 *Proc Natl Acad Sci USA* **113**:E2066-E2072.
- 399 11. **Gibiansky ML, Conrad JC, Jin F, Gordon VD, Motto DA, Mathewson MA, Stopka WG,**
400 **Zelasko DC, ShROUT JD, Wong GC.** 2010. Bacteria use type IV pili to walk upright and detach
401 from surfaces. *Science* **330**:197-197.
- 402 12. **Pratt LA, Kolter R.** 1998. Genetic analysis of *Escherichia coli* biofilm formation: roles of
403 flagella, motility, chemotaxis and type I pili. *Mol Microbiol* **30**:285-293.
- 404 13. **Purevdorj B, Costerton J, Stoodley P.** 2002. Influence of hydrodynamics and cell signaling on
405 the structure and behavior of *Pseudomonas aeruginosa* biofilms. *Appl Environ Microbiol*
406 **68**:4457-4464.
- 407 14. **Stoodley P, Cargo R, Rupp C, Wilson S, Klapper I.** 2002. Biofilm material properties as
408 related to shear-induced deformation and detachment phenomena. *J Ind Microbiol Biot* **29**:361-

- 409 367.
- 410 15. **Lecuyer S, Rusconi R, Shen Y, Forsyth A, Vlamakis H, Kolter R, Stone HA.** 2011. Shear
411 stress increases the residence time of adhesion of *Pseudomonas aeruginosa*. *Biophys J* **100**:341-
412 350.
- 413 16. **Nejadnik MR, Van Der Mei HC, Busscher HJ, Norde W.** 2008. Determination of the shear
414 force at the balance between bacterial attachment and detachment in weak-adherence systems,
415 using a flow displacement chamber. *Appl Environ Microbiol* **74**:916-919.
- 416 17. **Kostenko V, Salek MM, Sattari P, Martinuzzi RJ.** 2010. *Staphylococcus aureus* biofilm
417 formation and tolerance to antibiotics in response to oscillatory shear stresses of physiological
418 levels. *FEMS Immunol Med Mic* **59**:421-431.
- 419 18. **Persat A, Nadell CD, Kim MK, Ingremeau F, Siryaporn A, Drescher K, Wingreen NS,
420 Bassler BL, Gitai Z, Stone HA.** 2015. The mechanical world of bacteria. *Cell* **161**:988-997.
- 421 19. **Lelièvre C, Legentilhomme P, Gaucher C, Legrand J, Faille C, Bénézech T.** 2002. Cleaning
422 in place: effect of local wall shear stress variation on bacterial removal from stainless steel
423 equipment. *Chem Eng Sci* **57**:1287-1297.
- 424 20. **Wang L, Fan D, Chen W, Terentjev EM.** 2015. Bacterial growth, detachment and cell size
425 control on polyethylene terephthalate surfaces. *Sci Rep* **5**.
- 426 21. **Shirakura A, Nakaya M, Koga Y, Kodama H, Hasebe T, Suzuki T.** 2006. Diamond-like
427 carbon films for PET bottles and medical applications. *Thin Solid Films* **494**:84-91.
- 428 22. **Li P, Cai X, Wang D, Chen S, Yuan J, Li L, Shen J.** 2013. Hemocompatibility and anti-
429 biofouling property improvement of poly (ethylene terephthalate) via self-polymerization of
430 dopamine and covalent graft of zwitterionic cysteine. *Colloid Surface B* **110**:327-332.
- 431 23. **Northen H, Paterson G, Constantino-Casas F, Bryant C, Clare S, Mastroeni P, Peters S,
432 Maskell D.** 2010. *Salmonella enterica* serovar typhimurium mutants completely lacking the

- 433 F0F1 ATPase are novel live attenuated vaccine strains. *Vaccine* **28**:940-949.
- 434 24. **Defoirdt T, Miyamoto CM, Wood TK, Meighen EA, Sorgeloos P, Verstraete W, Bossier P.**
435 2007. The natural furanone (5Z)-4-bromo-5-(bromomethylene)-3-butyl-2 (5H)-furanone disrupts
436 quorum sensing-regulated gene expression in *Vibrio harveyi* by decreasing the DNA-binding
437 activity of the transcriptional regulator protein LuxR. *Environ Microbiol* **9**:2486-2495.
- 438 25. **Jayaraman A, Wood TK.** 2008. Bacterial quorum sensing: signals, circuits, and implications for
439 biofilms and disease. *Annu Rev Biomed Eng* **10**:145-167.
- 440 26. **García AJ, Ducheyne P, Boettiger D.** 1997. Quantification of cell adhesion using a spinning
441 disc device and application to surface-reactive materials. *Biomaterials* **18**:1091-1098.
- 442 27. **Fitts MK, Pike DB, Anderson K, Shiu Y-T.** 2014. Hemodynamic shear stress and endothelial
443 dysfunction in hemodialysis access. *Open Urol Nephrol J* **7**:33.
- 444 28. **Mukherjee PK, Chand DV, Chandra J, Anderson JM, Ghannoum MA.** 2009. Shear stress
445 modulates the thickness and architecture of *Candida albicans* biofilms in a phase-dependent
446 manner. *Mycoses* **52**:440-446.
- 447 29. **Cookson AL, Cooley WA, Woodward MJ.** 2002. The role of type 1 and curli fimbriae of Shiga
448 toxin-producing *Escherichia coli* in adherence to abiotic surfaces. *Int J Med Microbiol* **292**:195-
449 205.
- 450 30. **Rolfe MD, Rice CJ, Lucchini S, Pin C, Thompson A, Cameron AD, Alston M, Stringer MF,**
451 **Betts RP, Baranyi J.** 2012. Lag phase is a distinct growth phase that prepares bacteria for
452 exponential growth and involves transient metal accumulation. *J Bacteriol* **194**:686-701.
- 453 31. **Weart RB, Levin PA.** 2003. Growth rate-dependent regulation of medial FtsZ ring formation. *J*
454 *Bacteriol* **185**:2826-2834.
- 455 32. **Weart RB, Lee AH, Chien A-C, Haeusser DP, Hill NS, Levin PA.** 2007. A metabolic sensor
456 governing cell size in bacteria. *Cell* **130**:335-347.

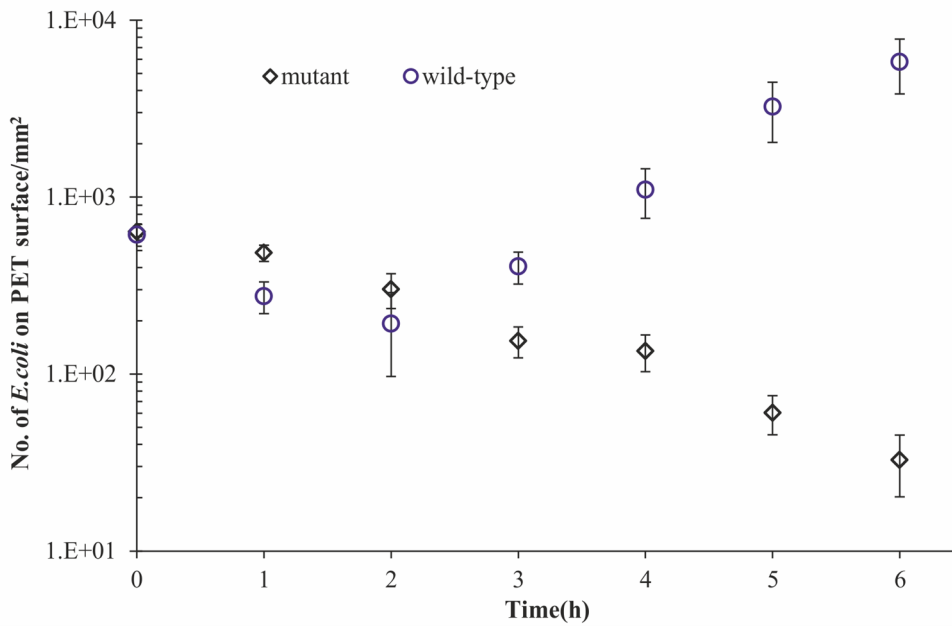
- 457 33. **Otto K, Norbeck J, Larsson T, Karlsson K-A, Hermansson M.** 2001. Adhesion of type 1-
458 fimbriated *Escherichia coli* to abiotic surfaces leads to altered composition of outer membrane
459 proteins. *J Bacteriol* **183**:2445-2453.
- 460 34. **Lazazzera BA.** 2005. Lessons from DNA microarray analysis: the gene expression profile of
461 biofilms. *Curr Opin Microbiol* **8**:222-227.
- 462 35. **De La Fuente L, Montanes E, Meng Y, Li Y, Burr TJ, Hoch H, Wu M.** 2007. Assessing
463 adhesion forces of type I and type IV pili of *Xylella fastidiosa* bacteria by use of a microfluidic
464 flow chamber. *Appl Environ Microbiol* **73**:2690-2696.
- 465 36. **Boks NP, Norde W, van der Mei HC, Busscher HJ.** 2008. Forces involved in bacterial
466 adhesion to hydrophilic and hydrophobic surfaces. *Microbiology+* **154**:3122-3133.
- 467 37. **Otto M.** 2014. Physical stress and bacterial colonization. *FEMS Microbiol Rev* **38**:1250-1270.
- 468 38. **Silhavy TJ, Kahne D, Walker S.** 2010. The bacterial cell envelope. *CSH Perspect Biol*
469 **2**:a000414.
- 470 39. **Peterson BW, Sharma PK, van der Mei HC, Busscher HJ.** 2012. Bacterial cell surface
471 damage due to centrifugal compaction. *Appl Environ Microbiol* **78**:120-125.
- 472 40. **Tsakalidou E, Papadimitriou K.** 2011. Stress responses of lactic acid bacteria. Springer Science
473 & Business Media.
- 474
475
476

477 **Figures**



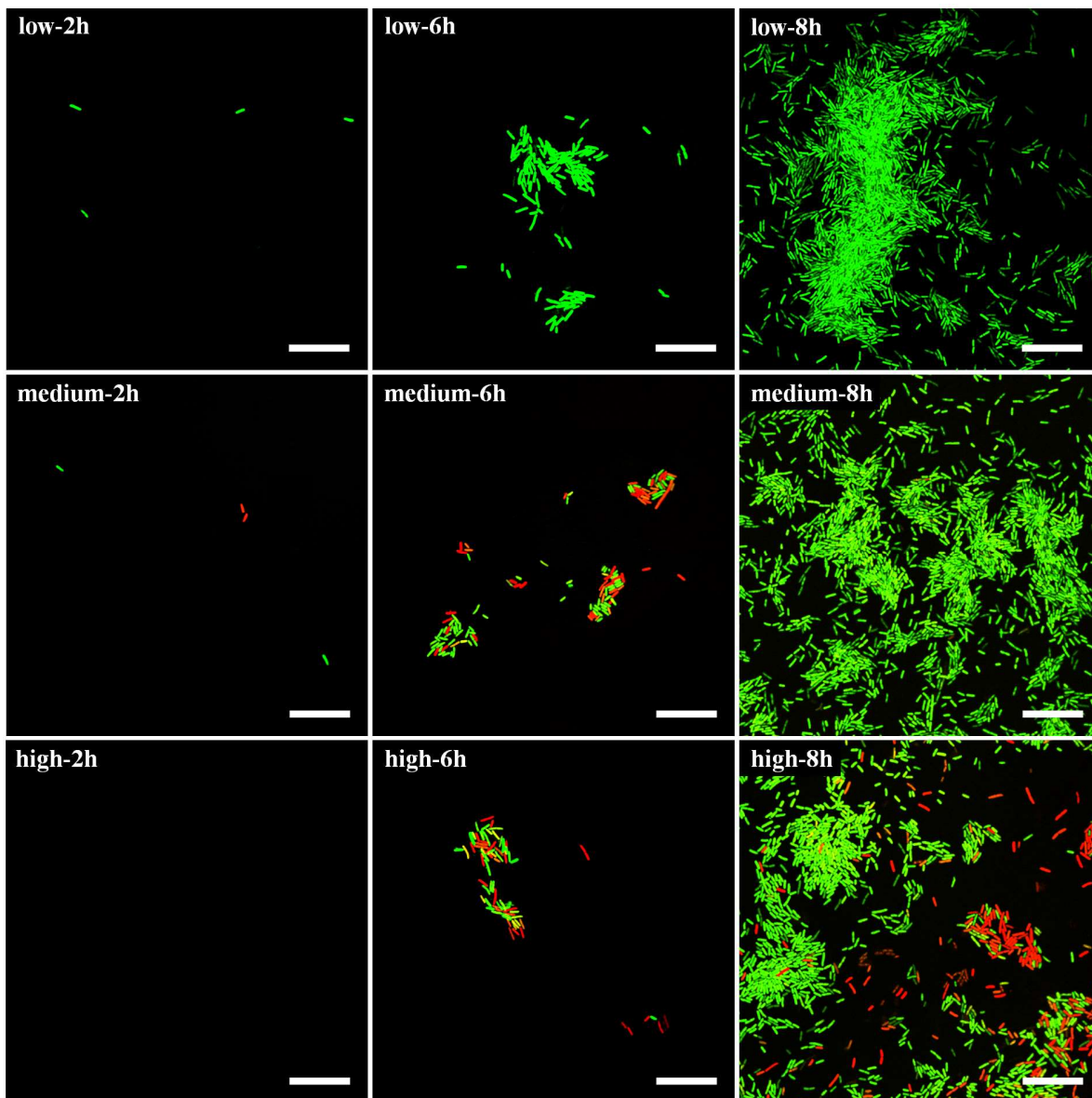
478

479 Fig.1 CLSM fluorescence images of *E.coli* *ΔfimA* mutant cells (labeled as *ΔfimA*) and wild-type *E. coli*
480 cells (labeled as WT) on PET surfaces at each hour interval. 0 h represents the initial 'seeded' bacteria
481 after PET surfaces were incubated with bacterial suspension of *ΔfimA* mutants or wild-type cells for 1 h.
482 Cells with intact and compromised membranes are stained with green and red, respectively.



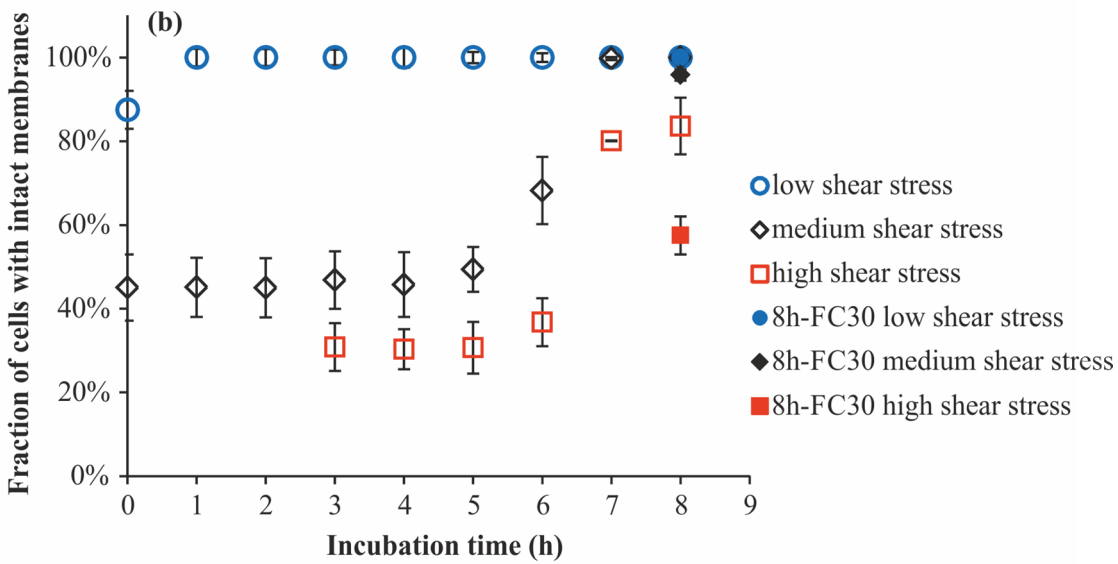
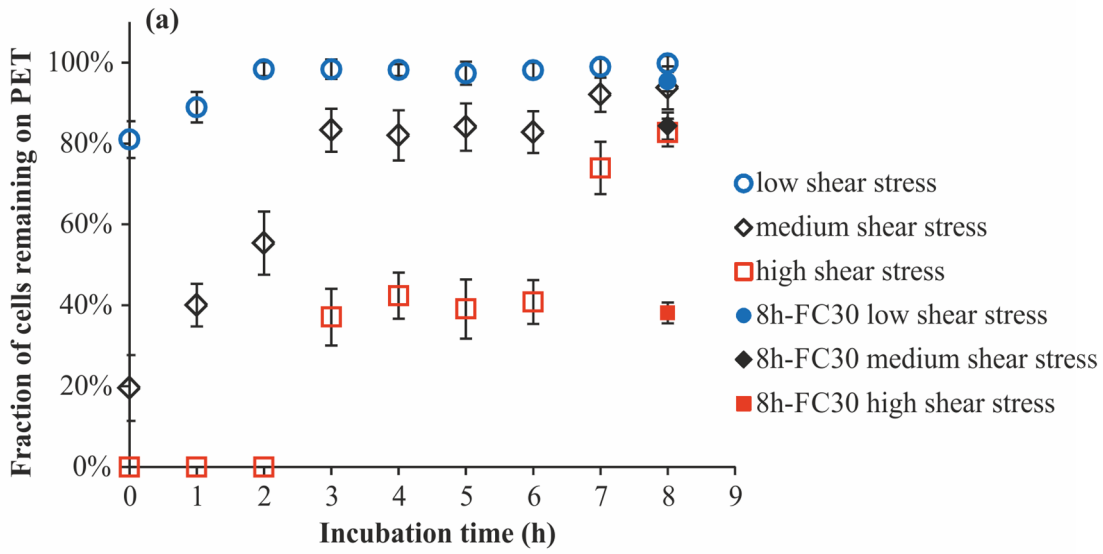
483

484 Fig.2 The number of *ΔfimA* mutants (black) and that of wild-type cells (blue) on PET surfaces after
 485 incubation with refreshed external LB medium. The data at 0 h refer to the respective number of the
 486 initially ‘seeded’ *ΔfimA* mutants and the wild-type *E.coli*. The wild-type results are presented in our
 487 previous study (20), shown here for comparison.



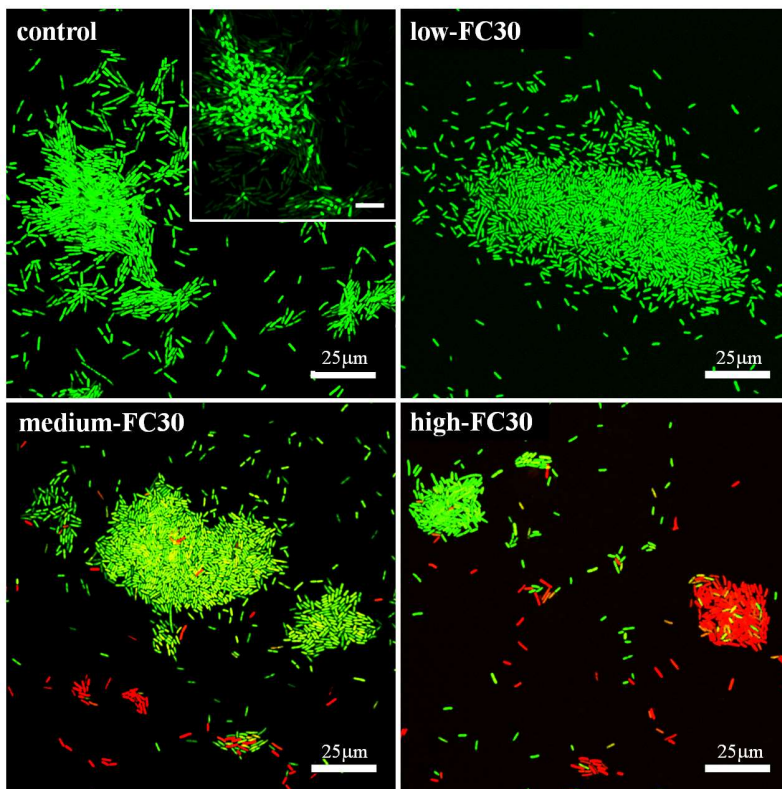
488

489 Fig.3 CLSM fluorescence images of wild-type *E.coli* MG1655 on PET surfaces, which were incubated
 490 with refreshed external LB medium for 2, 6 and 8 h, and then challenged for 120s with low, medium and
 491 high shear stress, respectively. Scale bar: 25 μ m. Cells with intact and compromised membranes are
 492 stained with green and red, respectively.



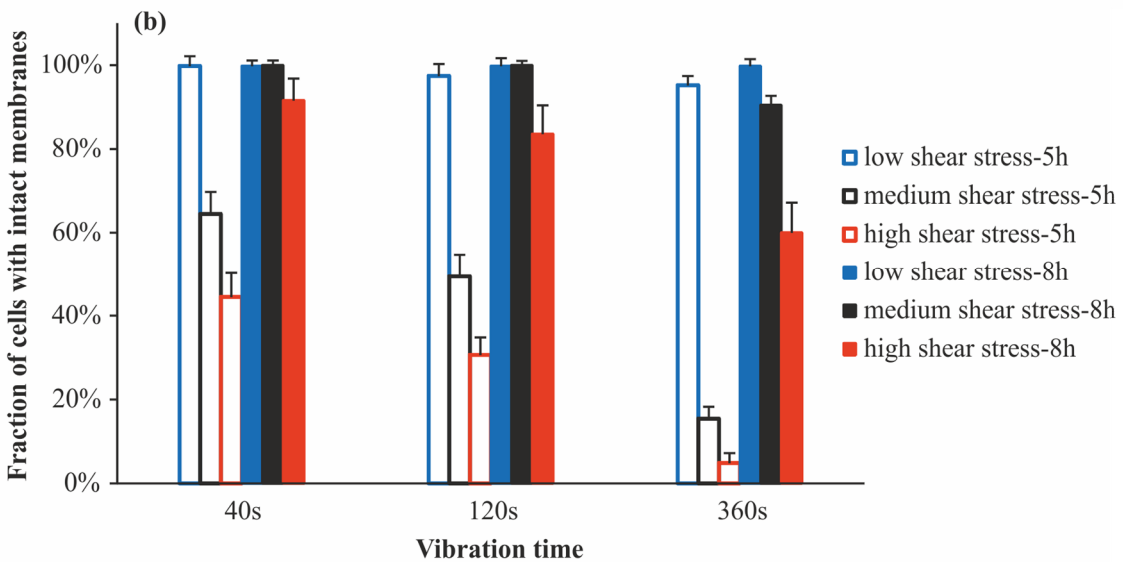
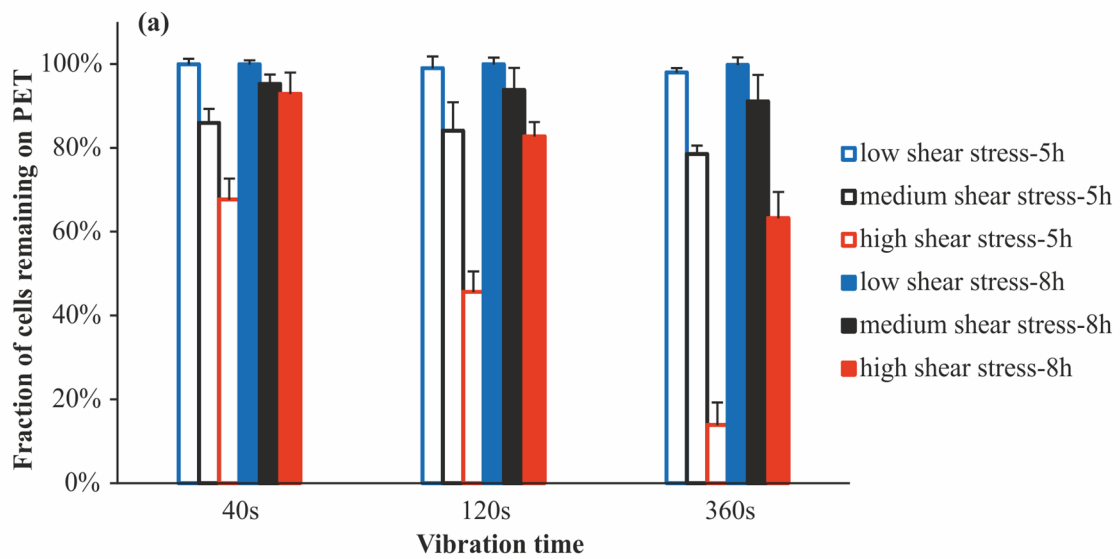
493

494 Fig.4 (a) The fraction of wild-type *E.coli* MG1655 remaining on PET surfaces after application of low,
 495 medium and high shear stress for 120 s. (b) The corresponding fraction of cells with intact membranes
 496 accounting for total cells remaining on surfaces. The data at 0 h refer to the initially ‘seeded’ *E.coli* after
 497 fluid shear treatment.



498

499 Fig. 5 CLSM fluorescence images of *E.coli* MG1655 cells, which grew on PET surfaces for 8 h with
 500 quorum sensing inhibited by quorum inhibitor (FC30) and then were respectively treated by low,
 501 medium and high shear stress for 120 s. Control: bacteria grew on PET surfaces under unstressed
 502 condition for 8 h without quorum sensing inhibited (the inset shows the upper layer of cells in the
 503 multilayer colony, when they are put in focus using CLSM 3D-scanning-mode, and the inset scale bar is
 504 10 μm). Cells with intact and compromised membranes are stained with green and red, respectively.



505

506 Fig.6 (a) The fraction of *E.coli* MG1655 remaining on PET surfaces after application of low, medium
 507 and high shear stress for 40, 120 and 360 s. (b) The corresponding fraction of cells with intact
 508 membranes accounting for total cells remaining on surfaces.